calculated quadrupole splitting at each temperature is shown as a solid line in Fig. 5(a). In Fig. 6(a) six lower levels give large positive quadrupole splittings which decrease a little as one goes to more excited states. The higher excited states contribute negative quadrupole splittings, but their energy levels are so high that they are not occupied at ordinary temperatures. The spin-orbit ground state is a doublet, $Y_2^2\chi_2$ and $Y_2^{-2}\chi_{-2}$. The application of the crystal field theory to Fe^{57} in Ca(II) site meets some difficulties, especially because of the limitation of the point-charge approximation and the lack of symmetry of Ca(II) sites. The charges of Ca and F ions are expected to be nearly equal to $+2$ and -1, respectively, but those of P and O in PO_4^{3-} are uncertain. According to Pauling's estimate[18] P has a charge of $+0.85$, which means a charge of -0.96 for the oxygen ion. Calculation of the electric field gradient using these values did not give the c axis as the direction of the maximum electric field gradient. This is not in accord with experimental observation. However, if the charge of the oxygen ion is increased to -1.25, then the c axis is the direction of the maximum electric-field gradient. Using free-ion values[14] 4.51 and 1.39 as $\langle r^4\rangle$ and $\langle r^2\rangle$, respectively, we carried out crystal field calculation for orbital states only, and the results are shown in Fig. 6(b). The lower two levels contribute positive values to V_{zz} while the higher three levels contribute negative values. However, since the crystal field splittings are comparable to spin-orbit coupling, we can expect to have small quadrupole splittings and a rapid temperature dependence because of heavy mixing of various orbital states by the spin-orbit coupling. The orbital ground state was found to be

$$(-0.245-0.662i)Y_2^2+(-0.033+0.049i)Y_2^0 +(0.705-0.028i)Y_2^{-2}.$$

[18] L. Pauling, *The Nature of the Chemical Bond* (Cornell University Press, Ithaca, N. Y., 1960), p. 322.

ACKNOWLEDGMENTS

The author would like to express his sincere thanks to Professor R. Smoluchowski for his support of this work and for his reading of the manuscript. Thanks must be extended to Professor B. S. H. Royce for his support and useful suggestions, and to Professor R. C. Axtmann, Professor T. D. Thomas, and Dr. Y. Hazony for the use of their equipment. The author is also indebted to John W. Hurley for his earnest cooperation in the experiment.

PHYSICAL REVIEW VOLUME 185, NUMBER 2 10 SEPTEMBER 1969

Antiferromagnetic Resonance and Mn^{55} Nuclear Magnetic Resonance in Cobalt-Doped $RbMnF_3$

W. J. INCE,* D. GABBE, AND A. LINZ

Department of Electrical Engineering and Center for Materials Science and Engineering, Massachusetts Institute of Technology, Cambridge, Massachusetts 02173

(Received 4 April 1969)

Single crystals of Co-doped $RbMnF_3$ have been grown by the Czochralski method, with doping concentrations ranging from zero to about 1500 ppm. It is found from antiferromagnetic-resonance (AFMR) measurements that the crystalline cubic anisotropy constant K_1 varies in a fairly linear manner with Co concentration. There appears to be little or no increase in K_2. The constant K_1 becomes zero at about 340-ppm Co concentration. AFMR and Mn^{55} nuclear resonance have been investigated experimentally over a wide frequency range. The data agree well with the computed mode spectra. The results imply that the sublattice magnetizations and the exchange and effective nuclear hyperfine fields are essentially unaffected by the presence of the Co. Some additional modes have been observed which are not predicted by the theory.

I. INTRODUCTION

IT is well known[1] that the presence of small amounts of Co has a pronounced effect on the crystalline anisotropy of certain ferrites. The divalent cobalt ions enter into octahedral sites, replacing Fe^{3+} ions. Bickford *et al.*[2] have studied Co-substituted magnetite single crystals, $Co_xFe_{3-x}O_4(0\leq x\leq 0.04)$ in the temperature range 120–450°K. They found that the Co added a positive contribution to the cubic anisotropy constant K_1 and a negative one to K_2. The sign of K_1 could be changed from negative to positive by adding sufficient Co, the amount needed being a function of temperature. Eastman *et al.*[3] were able to vary the magnitude and sign of K_1 in the cubic antiferromagnet $TlMnF_3$ through the substitution of a small amount ($\leq$1000 ppm) of Co for divalent manganese. This earlier work suggested the possibility of similarly using Co substitu-

* Also Staff Associate, M.I.T. Lincoln Laboratory, Lexington, Mass.

[1] R. F. Pearson, J. Appl. Phys. **31**, 160S (1960).

[2] L. R. Bickford, Jr., *et al.*, Proc. IEE Suppl. No. 5 **104B**, 238 (1957).

[3] D. E. Eastman *et al.*, J. Appl. Phys. **38**, 5209 (1967).

tion to vary the magnitude and sign of K_1 in the cubic antiferromagnet $RbMnF_3$.

The magnetic properties of undoped $RbMnF_3$ have been well established by previous work.[4-8] Below the Néel temperature of 82.6°K, the divalent manganese ions form a two-sublattice system of electronic spins, the ⟨111⟩ axes being the easy directions of magnetization. The resonance characteristics of $RbMnF_3$ can be interpreted by assuming the anisotropy energy $\mathcal{H}_a$ to be given by just the first term in the following power series expansion:

$$\mathcal{H}_a=\tfrac{1}{2}\sum_{j=1,2}[K_1(\alpha_{1j}^2\alpha_{2j}^2+\alpha_{2j}^2\alpha_{3j}^2+\alpha_{3j}^2\alpha_{1j}^2)+K_2\alpha_{1j}^2\alpha_{2j}^2\alpha_{3j}^2+\cdots], \quad (1)$$

where the α_{1j}'s are the direction cosines of the electronic sublattice magnetizations.

Single crystals of $RbMn_{1-x}Co_xF_3$ have been prepared[9] with Co concentrations of up to about 1500 ppm. It was found that for the degree of doping used, the anisotropy constant varied in a roughly linear manner with doping concentration. The sign of K_1 could be changed from negative to positive, going through zero at a Co concentration of about 340 ppm. For the amounts of Co used, the effect of the impurity on the exchange field H_E, and the electronic sublattice magnetizations M_1 and M_2 was negligible.

The crystals were prepared by a method similar to that used for pure $RbMnF_3$. A method for preparing the pure $RbMnF_3$ feed has been described by Henk *et al.*[10] The basic starting materials are Rb carbonate, Mn carbonate, and hydrofluoric acid, which undergo the following reaction:

$$Rb_2CO_3+2MnCO_3+6HF\rightarrow 2RbMnF_3+3H_2O+CO_2. \quad (2)$$

The process is carried out via a number of intermediate steps, which include purification of the starting materials. The final product is dried in a dessicator over KOH, in order to remove excess hydrogen fluoride and water.

The Co additive was prepared from the appropriate amount of reagent grade Co carbonate, which was dissolved in a 48% solution of HF. The liquid was centrifuged to remove a small amount of insoluble residue, which was probably a mixture of Co oxides. The resulting supernatant solution of CoF_2 was decanted directly onto 150 g of pure $RbMnF_3$ feed, which was then dried in an atmosphere of HF.

$RbMn_{1-x}Co_xF_3$ crystals were grown from the melt by the Czochralski method. The starting seed was pure $RbMnF_3$. Altogether seven crystals were grown, having various dopant concentrations and averaging about 30 mm in length. Over this length, the concentration varied, typically, by about 10%, being greatest at the bottom of the boule. The concentration gradient in the plane transverse to the pulling axis was negligible.

AFMR and NMR experiments were performed at 4.2°K on single-crystal cubes of $RbMn_{1-x}Co_xF_3$, using standard cavity techniques. Each sample was cut from a plane perpendicular to the crystal growth axis which, for all crystals, was a ⟨100⟩ direction. Two cube faces were {100} planes and four were {110} planes, so that the sample could be rotated about either the [100] or the [110] axis. Samples of $RbMn_{1-x}Co_xF_3$ to be analyzed for Co were taken from the same plane as the working crystals. Weighed samples were dissolved directly in concentrated HCl without having been powdered. Fluoride was removed by repeated evaporations at 90°C with HCl. The residue consisting of $RbMn_{1-x}Co_xCl_3$ was dissolved in water and diluted to 50.00 ml. This solution provided sufficient material for duplicate analyses of each sample. The 2-nitroso-1-naphthol method[11] was used for analysis. The accuracy and precision of the analytic data are about ±5%. One crystal was analyzed by an independent method.[12] The results obtained by the two methods agreed to better than 1%.

The amount of Co-doping used did not appreciably disturb the cubic-crystal structure. The resonance characteristics of the doped crystals can be explained reasonably well by assuming that the anisotropy energy is still represented by the K_1 term of the power series expansion, Eq. (1). At low temperatures, $|\mathbf{M}_1|$ and $|\mathbf{M}_2|$ are unaffected by an applied field, i.e., the parallel susceptibility is negligible. Thus, $\mathcal{H}_a$ can be written as a function of the direction cosines α_1 of the vector $\mathbf{M}[=\frac{1}{2}(\mathbf{M}_1-\mathbf{M}_2)]$:

$$\mathcal{H}_a=K(\alpha_1^2\alpha_2^2+\alpha_2^2\alpha_3^2+\alpha_3^2\alpha_1^2). \quad (3)$$

When $0<x<0.00034$, K is negative, and the ⟨111⟩ axes are the easy directions of magnetization. For $x>0.00034$, K is positive and the ⟨100⟩ axes become the preferred directions.

Table I shows the measured values of the quantity $4K/3M$ for several crystals as a function of Co concentration. This choice of parameter is convenient, since $4|K|/3M$ is the effective anisotropy field H_A along an easy axis for negative K. We shall retain this definition of H_A for the case of positive K. For the crystal

[4] D. T. Teaney *et al.*, Phys. Rev. Letters **9**, 212 (1962).
[5] M. J. Freiser *et al.*, *Proceedings of the International Conference on Magnetism, Nottingham, 1964* (Institute of Physics and the Physical Society, London, 1965) p. 432.
[6] P. H. Cole and W. J. Ince, Phys. Rev. **150**, 377 (1966).
[7] A. J. Heeger and D. T. Teaney, J. Appl. Phys. **35**, 846 (1964).
[8] W. J. Ince, Ph.D. thesis, M.I.T., 1969.
[9] The crystals used throughout this work were grown in the Crystal Physics Laboratory, Center for Materials Science and Engineering, M.I.T.
[10] P. O. Henk, D. Gabbe, and K. Bangerskis, Tech. Memo No. 3, Microwave and Quantum Magnetics Group, Dept. of Electrical Engineering and Center for Materials Science and Engineering, M.I.T. (unpublished).
[11] E. B. Sandell, *Colorimetric Determination of Traces of Metals* (Wiley-Interscience, Inc., New York, 1959), 3rd ed., p. 420.
[12] The independant analysis was performed by Dr. E. B. Owens, M.I.T. Lincoln Laboratory.

TABLE I. Parameter $4K/3M$ versus Co concentration for various crystal specimens.

Co concentration (ppm)	$4K/3M$ (Oe)
0	−4.59
250	−1.16
280	−1.0
340	≈0
450	+1.18
520	+2.54
1450	+13.0

with 340-ppm nominal Co concentration, $4K/3M$ varied from −0.6 Oe at the bottom of the boule to 0.6 Oe at the top. The corresponding Co concentrations were 332 and 367 ppm, respectively, while the nominal figure pertained to the middle of the boule.

The anisotropy field of each crystal was obtained by either of two methods: (1) measurements of the fields for AFMR with the field applied along two different principal directions—usually the ⟨100⟩ and the ⟨110⟩ axes, and (2) extrapolation of the AFMR modes to zero applied field.

When plotted as a function of crystal orientation, the field for resonance exhibits twofold symmetry if the applied field $\mathbf{H}_0$ is in the (110) plane and fourfold symmetry in the (100) plane. Figures 1 and 2 show plots of the field for AFMR versus angle for samples having negative and positive K, respectively. With a given value of K, the type of plot is not, of course, unique. It is a function of the choice of frequency, relative to the AFMR frequency in zero applied field.

II. ANTIFERROMAGNETIC RESONANCE

The anisotropy constant is most rapidly obtained by measuring the field for AFMR for the field-dependent flopped mode as a function of crystal orientation. By choosing a sufficiently high frequency, the field for resonance is large enough to ensure spin-flop. $\mathbf{M}_1$ and $\mathbf{M}_2$ then lie in the plane orthogonal to $\mathbf{H}_0$, and point in the direction of minimum anisotropy within the plane. In the spin-flop configuration, the AFMR frequencies are given by particularly simple expressions.[5] They are

$$(\Omega_1/\Gamma)^2 = H_0^2 + 2H_E H_{NE} + 3H_E H_A f(\theta,\varphi), \quad (4)$$

$$(\Omega_2/\Gamma)^2 = 2H_E H_{NE} + 3H_E H_A g(\theta,\varphi). \quad (5)$$

In Eqs. (4) and (5), Γ is the electronic gyromagnetic ratio, H_{NE} is the effective hyperfine field acting on the electronic spins, and $f(\theta,\varphi)$, $g(\theta,\varphi)$ are functions of the spherical coordinate angles of $\mathbf{M}$ with respect to the crystal axes. The angles θ and φ are measured from the [001] and [100] axes, respectively.

Teaney *et al.*[4,5] first derived the flopped AFMR equations for pure $RbMnF_3$ ($K<0$). In their equations, the angular functions are expressed in terms of the direction angles (θ_H,φ_H) of $\mathbf{H}_0$. The field is restricted to either the (110) or the (100) plane. Eastman[3] has derived the corresponding angle functions for the case of positive K.

The exchange and anisotropy fields may be obtained separately from Eq. (4) by choosing two different directions for $\mathbf{H}_0$. For low anisotropy crystals, the term in Eq. (4) which contains H_A is small, and this method becomes rather inaccurate. Thus, alternatively, in the present work, the AFMR frequencies were measured as a function of field, with $\mathbf{H}_0$ applied parallel to one of the three principal axes of the crystal. The theoretical AFMR modes were then fitted to the experimental data by appropriate choice of H_E and H_A.

In order to calculate the resonant frequencies by the second method, it is necessary to know the orientation of the magnetic sublattices as a function of the applied field when $\mathbf{M}_1$ and $\mathbf{M}_2$ are not necessarily flopped.

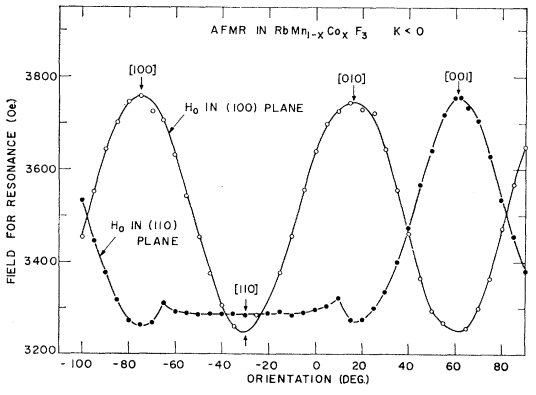

FIG. 1. Applied field for AFMR in $RbMn_{0.99975}Co_{0.00025}Fe_3$ versus crystal orientation. $4K/3M=-1.16$ Oe. Resonant frequency = 11.30 GHz.

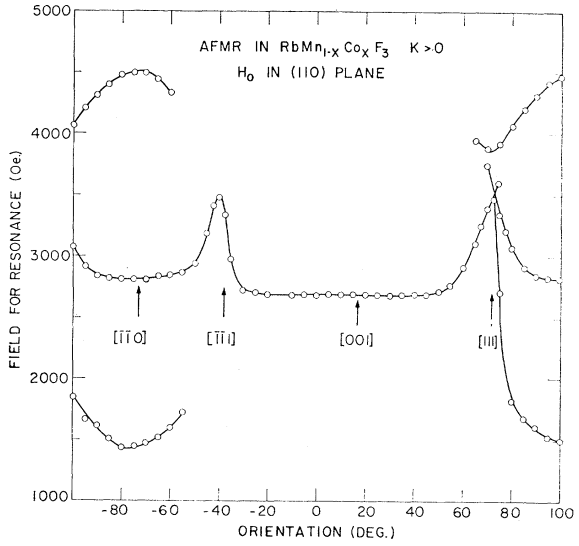

FIG. 2. Applied field for AFMR in $RbMn_{0.99948}Co_{0.00052}F_3$ versus crystal orientation. $4K/3M=2.54$ Oe. Resonant frequency = 11.593 GHz.

AFMR, $K<0$

If $\mathbf{M}$ and $\mathbf{H}_0$ both lie in the (110) plane, the direction of $\mathbf{M}$ is given by[6]

$$H_0^2 \sin 2(\theta-\theta_H) = (KH_E/M) \sin 2\theta\,(1+3\cos 2\theta). \quad (6)$$

Also, the AFMR frequencies are the solutions of the following equation:

$$(\omega^2-\Omega_+^2)(\omega^2-\Omega_-^2)-4(\Gamma H_0)^2\omega^2\cos^2(\theta-\theta_H)=0, \quad (7)$$

with

$$(\Omega_+/\Gamma)^2 \approx 2H_E[H_{NE}+\tfrac{3}{2}H_A f(\theta)] + H_0^2[2\sin^2(\theta-\theta_H)-1], \quad (8)$$

and

$$(\Omega_-/\Gamma)^2 \approx 2H_E[H_{NE}+\tfrac{3}{2}H_A g(\theta)] + H_0^2[\sin^2(\theta-\theta_H)-1], \quad (9)$$

where

$$f(\theta) = -(1-\tfrac{13}{2}\sin^2\theta+6\sin^4\theta), \quad (10)$$

$$g(\theta) = -(1-\tfrac{7}{2}\sin^2\theta+\tfrac{3}{2}\sin^4\theta). \quad (11)$$

When K is negative, the resonance behavior of Co-doped $RbMnF_3$ is similar to that of the pure material, except for a reduced value of H_A. If the field is applied in the [001] direction, $\mathbf{M}$ is constrained to rotate away from the easy axis, and for values of H_0 greater than $(\frac{3}{2}H_E H_A)^{1/2}$, the magnetization is flopped along the [110] axis. In the flopped configuration, the solutions to Eq. (7) become

$$(\Omega_1/\Gamma)_{[001]}^2 = H_0^2+2H_E H_{NE}-\tfrac{3}{2}H_E H_A, \quad (12)$$

$$(\Omega_2/\Gamma)_{[001]}^2 = 2H_E H_{NE}+3H_E H_A. \quad (13)$$

When $\mathbf{H}_0$ is parallel to the [111] axis, the threefold symmetry dictates that $\mathbf{M}$ lies in the (110) plane. The observed resonances imply that the direction of $\mathbf{M}$ corresponds to the absolute minimum in the free energy. The value of θ in Eqs. (10) and (11) lies between the limits $125.3°\leq\theta\leq144.7°$. If $\mathbf{H}_0$ is applied in the [110] direction, $\mathbf{M}$ remains flopped along either the $[\bar{1}11]$ or $[1\bar{1}1]$ axis for all values of applied field. The resonant frequencies are obtained from Eq. (7) by putting $(\theta-\theta_H)=90°$ and $\theta=54.7°$. The resonant frequencies are

$$(\Omega_1/\Gamma)_{[110]}^2 = H_0^2+2H_E(H_{NE}+H_A), \quad (14)$$

$$(\Omega_2/\Gamma)_{[110]}^2 = 2H_E(H_{NE}+H_A). \quad (15)$$

Another possible equilibrium direction of $\mathbf{M}$, which corresponds to a relative minimum in the free energy,[6] lies in the same (110) plane as $\mathbf{H}_0$. However, the equivalent resonances have not been observed in Co-doped crystals.

Figure 1 illustrates a typical plot of the applied field for AFMR versus crystal orientation, for a Co-doped sample of $RbMnF_3$ (250-ppm Co) having a negative anisotropy constant. The frequency of measurement

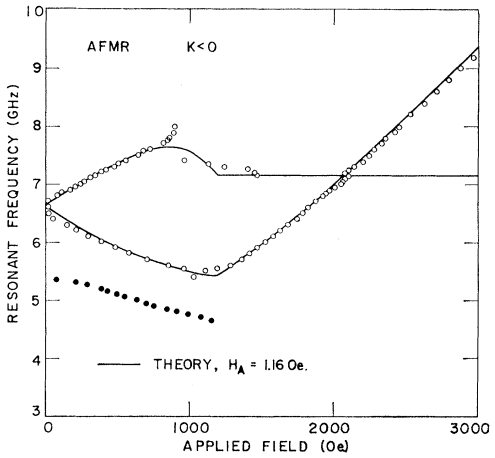

FIG. 3. AFMR in $RbMn_{0.99975}Co_{0.00025}F_3$ with $\mathbf{H}_0$ parallel to the [100] axis.

was 11.3 GHz. The applied field was large enough to ensure spin-flip when $\mathbf{H}_0$ was parallel to either the [100] or the [110] axis. In this case, H_A can be evaluated from Eqs. (12) and (14)

$$H_A = (2/7H_E)(H_{0[100]}^2 - H_{0[110]}^2) \quad (16)$$

and

$$H_E = \frac{3}{14H_{NE}}\left[\frac{7}{3}\left(\frac{\Omega_1}{\Gamma}\right)^2 - H_{0[110]}^2 - \tfrac{4}{3}H_{0[100]}^2\right]. \quad (17)$$

Assuming that H_{NE} has the same value as for pure $RbMnF_3$, i.e., $(9.43/T\ °K)$ Oe, Eq. (17) gives 8.12×10^5 Oe for H_E. This agrees, within experimental error, with the value of H_E for the pure material. By substituting for H_E in Eq. (16), H_A is found to be 1.12 Oe for this particular sample ($4K/3M=-1.12$ Oe).

Figure 3 shows the AFMR frequencies for

$$RbMn_{0.99975}Co_{0.00025}F_3,$$

plotted as a function of $\mathbf{H}_0$, with the field parallel to the [100] axis. Extrapolation of the mode branches to zero field gives the value of 1.16 Oe for H_A.

A third mode, shown in the figure, was detected experimentally. These additional resonances, which are not predicted by the theory, were weak and could only be tracked over a restricted range of applied field. The third AFMR mode was also visible when $\mathbf{H}_0$ was applied along a ⟨110⟩ axis. With the field in a ⟨111⟩ direction, only the two predicted modes were observed.

AFMR, $K>0$

When $K>0$, the AFMR characteristics differ markedly from the negative K case. We shall derive the resonant frequencies, with $\mathbf{H}_0$ parallel to one of the three principal axes.

The first case to be discussed is that of $\mathbf{H}_0$ applied in the [100] direction. There are three possible sublattice orientations, which give two pairs of resonant frequen-

cies. The magnetization can be flopped along either the [010] or the [001] axis, which are easy axes, regardless of the magnitude of $\mathbf{H}_0$. These directions have degenerate energies and yield only one pair of frequencies. These may be obtained from Eq. (7) by putting $(\theta-\theta_H)=90°$ and $\theta=0$. The angle functions for $f(\theta)$ and $g(\theta)$ become

$$f(0)=g(0)=1, \quad (K>0).$$

Thus, the resonant frequencies are

$$(\Omega_1/\Gamma)_{[100]}^2=H_0^2+2H_EH_{NE}+3H_EH_A, \tag{18}$$

$$(\Omega_2/\Gamma)_{[100]}^2=2H_EH_{NE}+3H_EH_A. \tag{19}$$

The other pair of frequencies corresponds to the condition that $\mathbf{M}$ and $\mathbf{H}_0$ are parallel. The frequencies are

$$\Omega_{1,2}/\Gamma=(2H_EH_{NE}+3H_EH_A)^{1/2}\pm H_0. \tag{20}$$

This configuration represents only a relative minimum in the free energy, and the resonances can be expected to be weaker than the pair given by Eqs. (18) and (19).

When $\mathbf{H}_0$ is parallel to the [110] axis, there are again three possible directions of $\mathbf{M}$, two of which yield identical frequencies. The equilibrium direction for $\mathbf{M}$ which represents the absolute minimum is the [001] axis, and $\mathbf{M}_1$ and $\mathbf{M}_2$ are in the flopped configuration. The corresponding resonant frequencies are given by Eqs. (18) and (19).

The two other equivalent positions are functions of $|\mathbf{H}_0|$. In zero applied field, they are the [100] and [010] axes. As the field strength is increased, $\mathbf{M}$ rotates away from either of these directions towards the perpendicular direction in the (001) plane. The appropriate transcendental equation, which gives the orientation of $\mathbf{M}$ as a function of $\mathbf{H}_0$, has been derived elsewhere,[8] and is

$$H_0^2\sin2(\varphi-\varphi_H)=\tfrac{3}{2}H_EH_A\sin4\varphi, \tag{21}$$

where φ and φ_H are the azimuthal angles of $\mathbf{M}$ and $\mathbf{H}_0$, respectively.

For spin-flop to occur in the (001) plane, we must have the condition $\varphi-\varphi_H=\frac{1}{2}\pi$, and Eq. (21) becomes

$$H_0^2=-3H_EH_A\sin2\varphi. \tag{22}$$

Further, if $\mathbf{H}_0$ is parallel to the [110] axis, the magnetization is flopped when $\varphi=-\frac{1}{4}\pi$, i.e., $H_0^2=3H_EH_A$. When $H_0^2<3H_EH_A$, the resonance frequencies may be obtained from Eq. (7) if $(\varphi-\varphi_H)$ is substituted for $(\theta-\theta_H)$ and also

$$f(\tfrac{1}{2}\pi,\varphi)=\cos4\varphi, \tag{23}$$

$$g(\tfrac{1}{2}\pi,\varphi)=\tfrac{1}{4}(3+\cos4\varphi). \tag{24}$$

When $H_0^2>3H_EH_A$, the following formulas hold:

$$(\Omega_1/\Gamma)_{[110]}^2=H_0^2+2H_EH_{NE}-3H_EH_A, \tag{25}$$

$$(\Omega_2/\Gamma)_{[110]}^2=2H_EH_{NE}+\tfrac{3}{2}H_EH_A. \tag{26}$$

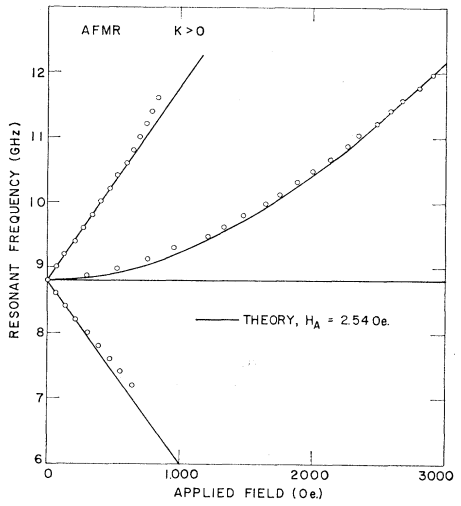

FIG. 4. AFMR in $RbMn_{0.99948}Co_{0.00052}F_3$ with $\mathbf{H}_0$ parallel to the [100] axis.

If $\mathbf{H}_0$ is applied along an axis of threefold symmetry, i.e., a ⟨111⟩ direction, only a single pair of resonances is expected. The magnetization is confined to the {110} planes, and is distributed statistically among the three domain orientations which correspond to minima in the free energy. As the field is increased, the magnetization rotates away from the easy axis, the direction of $\mathbf{M}$ in the (110) plane being given by Eq. (6). The resonant frequencies may be obtained from Eq. (7), with

$$f(\theta,\tfrac{1}{4}\pi)=(1-\tfrac{13}{2}\sin^2\theta+6\sin^4\theta), \tag{27}$$

$$g(\theta,\tfrac{1}{4}\pi)=1-\tfrac{7}{2}\sin^2\theta+\tfrac{3}{2}\sin^4\theta). \tag{28}$$

For this configuration, there is no definite spin-flop.

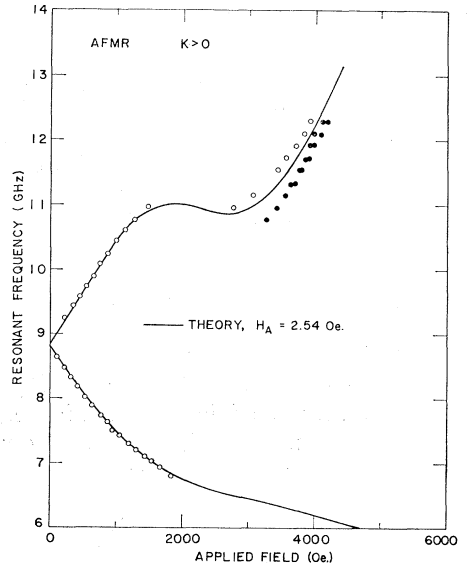

FIG. 5. AFMR in $RbMn_{0.99948}Co_{0.00052}F_3$ with $\mathbf{H}_0$ parallel to the [111] axis.

When K is positive, H_A may be obtained from experimental data, using the expressions for the field-tunable flopped resonances, Eqs. (18) and (25). Thus,

$$H_{0[110]}^2-H_{0[100]}^2=6H_EH_A, \quad (K>0). \tag{29}$$

Figure 4 shows the AFMR frequencies for

$$RbMn_{0.9994}Co_{0.00052}F_3$$

plotted against H_0, applied in the [100] direction. The theoretical curves were computed assuming H_A to be 2.54 Oe, which was determined from the measured zero-field frequency. Actually, a better fit to the experimental data was obtained by deriving H_A in this manner than by using Eq. (29). The flopped-tunable resonance was easily the most intense one. A general absorption in the vicinity of 8.8 GHz, caused by the field-independent mode, was also noted.

The two low-field branches, which correspond to the magnetization being aligned with $\mathbf{H}_0$, are of great interest. These resonances were weak, and died out at a field strength of about 800 Oe. The equivalent resonances in pure $RbMnF_3$, i.e., for $\mathbf{M}$ and $\mathbf{H}_0$ directed along the [111] axis, have not yet been observed.[6]

The AFMR modes for the same crystal ($K>0$, $H_A=2.54$ Oe), with $\mathbf{H}_0$ parallel to the [111] axis, are illustrated in Fig. 5. The rising branch exhibits an interesting maximum at a field of about 1800 Oe. It is caused by the relative variations of the anisotropy and Zeeman torques with the angle θ. For field strengths greater than 2000 Oe, the magnetization lies close to the $[11\bar{2}]$ direction, the low-frequency resonance becomes insensitive to the magnitude of the field and is difficult to detect. The high-frequency resonance line broke up into a triplet when H_0 exceeded 2000 Oe, indicating that there may have been some misalignment of the crystal.

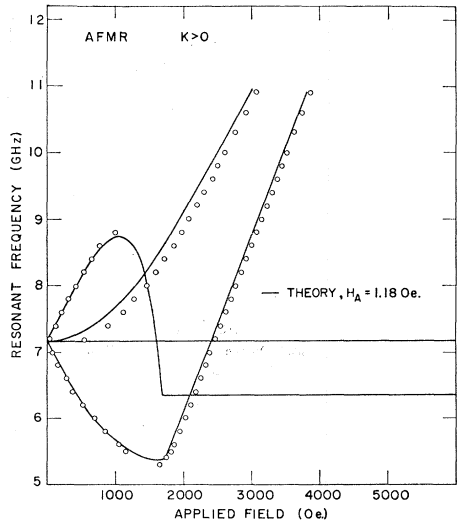

FIG. 6. AFMR in $RbMn_{0.99955}Co_{0.00045}F_3$ with $\mathbf{H}_0$ parallel to the [110] axis.

The resonance spectrum with the field applied in the [110] direction is shown in Fig. 6 for a sample of $RbMn_{0.99955}Co_{0.00045}F_3$. The value for H_A was 1.18 Oe ($K>0$). The flopped resonances, corresponding to $\mathbf{M}$ aligned in the [001] direction, were the most intense. The lack of agreement between the theoretical curves and the experimental points for this mode is too large to be accounted for by crystal misalignment.

The second set of resonances shown in Fig. 6, for which $\mathbf{M}$ and $\mathbf{H}_0$ lie in the same {100} plane, is very similar in character to Fig. 3. For both of these figures, the minimum frequency is $\Gamma(2H_EH_{NE})^{1/2}$ and the field at the crossover point is equal to $(\frac{9}{2}H_EH_A)^{1/2}$.

III. Mn^{55} NUCLEAR RESONANCE

In $RbMnF_3$, the electronic and nuclear spins of the Mn^{2+} ions are strongly coupled via the hyperfine interaction. Thus, the NMR frequencies are largely determined by the precession of the electronic moments. The measurement of the NMR frequency provides therefore an indirect means of determining the anisotropy constant.

In static equilibrium, the Mn nuclear moments are parallel to the electronic magnetization and behave, from the macroscopic viewpoint, as comprising two nuclear sublattices. Thus, there are two nuclear modes of frequencies $\omega_{1,2}$. In the flopped configuration, the nuclear frequencies are given by the relationship

$$\omega_{1,2}^2\approx\omega_N^2\left(1-\frac{2\Gamma^2H_{NE}H_E}{\Omega_{1,2}^2}\right), \tag{30}$$

where $\Omega_{1,2}$ are the electronic resonant frequencies and ω_N is the unpulled hyperfine frequency.[7] If the applied field is less than the value required to flop the magnetization, Eq. (30) does not apply. In this case, the nuclear frequencies have been derived[8] using a model comprising a total of four magnetic sublattices—two electronic and two nuclear. The coupled equations of motion for the four-sublattice system were solved, taking into account the instantaneous electron-nuclear correlation.

The unpulled hyperfine frequency, which is proportional to the strength of the hyperfine interaction, is the frequency of the field-tunable nuclear mode[7] extrapolated to infinite field strength. Thus, the values of ω_N obtained from experimental measurements enable one to examine the strength of the hyperfine interaction as a function of Co concentration. The unpulled hyperfine frequency can also be determined from double resonance experiments.[13] Mn^{55} nuclear resonance in Co-doped $RbMnF_3$ has been studied experimentally by both double resonance and direct methods. These experiments have confirmed that for the range of con-

[13] W. J. Ince, Phys. Rev. 177, 1005 (1969).

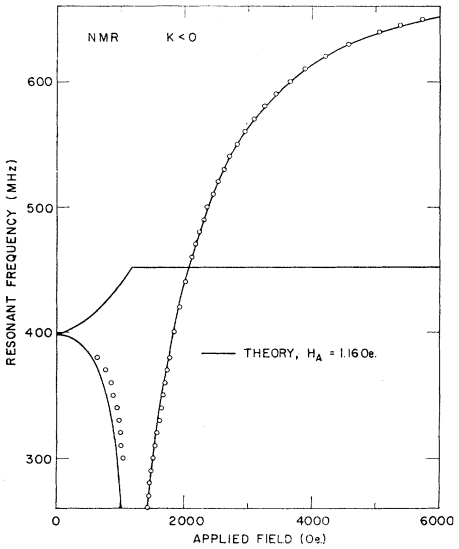

FIG. 7. Mn^{55} nuclear resonance in $RbMn_{0.99975}Co_{0.00025}F_3$ with $\mathbf{H}_0$ parallel to the [100] axis.

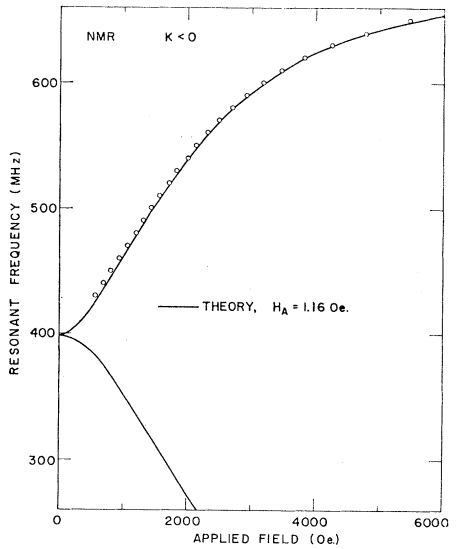

FIG. 8. Mn^{55} nuclear resonance in $RbMn_{0.99975}Co_{0.00025}F_3$ with $\mathbf{H}_0$ parallel to the [111] axis.

centrations used, the doping has negligible effect on the internal nuclear hyperfine interaction. In computing nuclear-resonant frequencies, ω_N was assumed to be[5] 686.2 MHz.

Direct NMR experiments were performed over the frequency range 250–687 MHz, using a shorted tunable TEM coaxial cavity. The signal was monitored using dc detection, with pen recorder or oscilloscope display. This simple arrangement was possible because, over most of the range of $|\mathbf{H}_0|$, the effective nuclear rf drive was enhanced through the motion of the electronic spins at the drive frequency.[7,8] In the flopped configuration, the field-independent nuclear mode is excited by applying the rf signal parallel to the steady field. Thus, there is no enhancement and this mode is not detectable. Below spin-flop, at least one mode could be tracked.

The results for a crystal having a negative anisotropy constant ($x=250$ ppm) are illustrated by Fig. 7. The theoretical curves were computed from the four-sublattice analysis, assuming $4K/3M$ to be -1.16 Oe. The flopped mode could be tracked over the entire frequency range available. Below spin-flop, the low-frequency branch could be followed over a limited-frequency range, but the sensitivity was insufficient to detect the high-frequency branch. With the field in the [111] direction (Fig. 8) only the high-frequency branch could be observed, due to the lack of sensitivity.

The resonances for a crystal having positive K ($x=450$ ppm) are shown in Fig. 9. For this example, H_A is equal to 1.18 Oe. When $\mathbf{H}_0$ was applied in either the [100] or the [110] direction, it was possible to detect only those resonances which corresponded to the magnetization being along the orthogonal [001] axis.

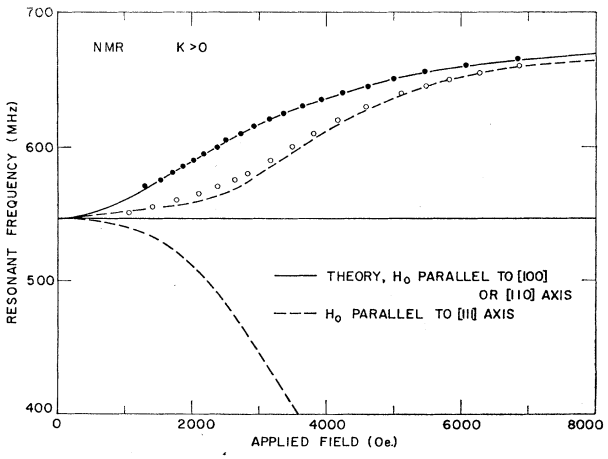

FIG. 9. Mn^{55} nuclear resonance in $RbMn_{0.99955}Co_{0.00045}F_3$. The theoretical curves were computed assuming $H_A=1.180$ Oe.

The [111] resonances are also shown in Fig. 9. Again, for the latter configuration, only the high-frequency branch was observed.

IV. DISCUSSION

The experimental data establish that the crystalline anisotropy of $RbMnF_3$ is markedly altered by the addition of small amounts of Co. For example, with a Co concentration of 1450 ppm, $4K/3M$ is changed from approximately -4.6 to $+13$ Oe. The corresponding Co contribution to K is 0.77 cm^{-1} per ion (4×10^3 ergs/cm^3), compared with 1.5 cm^{-1} per ion obtained by Eastman *et al.*, for Co-doped $TlMnF_3$. In pure $RbMnF_3$, the Mn^{2+} ions contribute only 4×10^{-4} cm^{-1} per ion (1.05×10^3 ergs/cm^3).

The doping level is sufficiently small that on the average the Co^{2+} ions are well separated from each other. The impurity ions act as pinning centers for the bulk magnetization. The Mn^{2+} spins are constrained by the exchange field to align with the cobalt spins, which therefore dictate the orientation of the net magnetization in static equilibrium. However, the response of the Mn^{2+} spins to an rf excitation is much the same as in the pure material.

The large contribution of the Co anisotropy is apparently due to the orbital degeneracy of the ground state of the Co^{2+} ion in the cubic crystalline field. The ground state of the free ion is ^4F, which splits into Γ_2, Γ_4, and Γ_5 levels in the cubic environment, with the Γ_4 level lowest. Van Vleck[14] has indicated that large magnetic anisotropy is to be expected if a degenerate level, such as Γ_4 or Γ_5, is lowest. Any other crystal-field component having lower than cubic symmetry will remove the degeneracy, thus introducing anisotropy. AFMR experiments on pure $RbMnF_3$ demonstrate that the anisotropy is cubic, to a good approximation. However, for the doped crystals, there is some indication of departure from cubic symmetry. In Figs. 3 and 6, for example, a zero-field splitting is discernible.

The effect of Co doping on the anisotropy of $RbMnF_3$ appears to be quite similar to that of magnetite,[2] as far as K_1 is concerned. However, in the case of $RbMnF_3$, there does not appear to be any significant increase in K_2 caused by the addition of the cobalt.

Slonczewski[15] has given an explanation for the magnetic anisotropy of Co-substituted magnetite. This material has cubic symmetry, with a small trigonal distortion. A basic assumption of Slonczewski's theory is that the lowest orbital level of Co^{2+} in the crystal field (cubic+trigonal) is doubly degenerate. The orbital angular momentum for these states is parallel to a $\langle111\rangle$ axis. The spin-orbit interaction gives rise to the observed anisotropy. The interaction energy can be written as $-\lambda LS|\cos\theta|$, where θ is the angle between the magnetization and the trigonal axis. Thus, the Co contribution to the free energy is maximum along the $\langle111\rangle$ axes, since λ is negative (-180 cm^{-1}).

Despite the general agreement between the computed and experimental AFMR spectra, some resonances which are not predicted by the theory have been observed. Consider, for example, the anomalous mode designated by the solid points in Fig. 3. This mode could be followed down to a frequency of 4.6 GHz, corresponding to a field strength of 1200 Oe in the [100] direction. At higher field values, the resonance absorption fell below the detection limit. A smooth curve drawn through the experimental points extrapolates to a frequency of 5.4 GHz in zero field. This is also the minimum frequency of the theoretical curve shown in Fig. 3, and represents the frequency shift $\Gamma(2H_EH_{NE})^{1/2}$ caused by the nuclear hyperfine interaction of the Mn^{2+} ions. Thus, frequencies lower than 5.4 GHz cannot be explained by the model. However, since the hyperfine interaction[16] in Co^{2+} is only about half that for Mn^{2+}, it is possible that the anomalous mode is due to the cobalt ions. Localized modes due to impurity spins have been observed in other materials.[17]

The cubic samples used in this work were 3 to 4 mm in length. Thus, the estimated anisotropy variation over the sample was about 1%. The increase in the flopped AFMR linewidth ΔH due to nonuniform anisotropy is approximately

$$\Delta H=(2\Gamma)^{-1}(\Delta H_A/H_A)\Omega_1.$$

This is about 20 Oe at X band. In fact, the observed linewidth was not appreciably greater than that of pure $RbMnF_3$.

ACKNOWLEDGMENTS

We wish to thank R. Mills for growing the crystals used in this work, and for x-ray analysis and crystal orientation. We are pleased to acknowledge helpful discussions with Professor F. R. Morgenthaler and Professor D. J. Epstein. A. Platzker assisted with some of the measurements.

[14] J. H. Van Vleck, Discussions Faraday Soc. **26**, 96 (1958).
[15] J. C. Slonczewski, Phys. Rev. **110**, 1341 (1958).
[16] R. E. Watson and A. J. Freeman, Phys. Rev. **123**, 2027 (1961).
[17] M. Motokawa and M. Date, J. Phys. Soc. Japan, **23**, 1216 (1967).